coatings

MDPI

Article

Transport of Magnetic Polyelectrolyte Capsules in Various Environments

Carmen Stavarache [1,2,*], Mircea Vinatoru [3] and Timothy Mason [2]

[1] "Costin D. Nenitescu" Institute of Organic Chemistry, 202B Splaiul Independentei, 060023 Bucharest, Romania
[2] Faculty of Health and Life Sciences, Coventry University, Priory Street, Coventry CV1 5FB, UK; apx077@coventry.ac.uk
[3] Sonochem Centre Ltd., Bank Gallery, High Street, Kenilworth CV8 1LY, UK; mircea@sonochemcentre.com
* Correspondence: stavarachec@yahoo.com; Tel.: +40-213167900; Fax: +40-213121601

Abstract: Microcapsules consisting of eleven layers of polyelectrolyte and one layer of iron oxide nanoparticles were fabricated. Two types of nanoparticles were inserted as one of the layers within the microcapsule's walls: Fe_2O_3, ferric oxide, having a mean diameter (Ø) of 50 nm and superparamagnetic Fe_3O_4 having Ø 15 nm. The microcapsules were suspended in liquid environments at a concentration of 10^8 caps/mL. The suspensions were pumped through a tube over a permanent magnet, and the accumulation within a minute was more than 90% of the initial concentration. The design of the capsules, the amount of iron embedded in the microcapsule, and the viscosity of the transportation fluid had a rather small influence on the accumulation capacity. Magnetic microcapsules have broad applications from cancer treatment to molecular communication.

Keywords: polyelectrolyte magnetic capsules; transport; drug delivery; molecular communication

check for updates

Citation: Stavarache, C.; Vinatoru, M.; Mason, T. Transport of Magnetic Polyelectrolyte Capsules in Various Environments. *Coatings* **2022**, *12*, 259. https://doi.org/10.3390/coatings12020259

Academic Editor: Cédric C. Buron

Received: 20 December 2021
Accepted: 13 February 2022
Published: 15 February 2022

Publisher's Note: MDPI stays neutral with regard to jurisdictional claims in published maps and institutional affiliations.

1. Introduction

Drug delivery systems are formulations or medical devices designed to transport the therapeutic agent to the specific site where it is needed (organ, tissue), followed by controlled release, in a reduced dose, thus minimizing undesirable side effects [1–3]. Numerous types of delivery systems, including liposomes, carbon nanotubes, micelles, dendrimers, and nanofibers, are under investigation as cytotoxic drug carriers [4,5]. Biopolymers such as animal-originated proteins and plant-originated carbohydrates are biocompatible, biodegradable, and antibacterial and thus also suited as drug carriers [6,7].

Polyelectrolyte capsules (PEs) are versatile drug carriers due to their constitution and properties [8,9]. Their fabrication involves a layer-by-layer technique: the construction of shells by alternating adsorption of oppositely charged polymers, either of natural origin (nucleic acids [10,11], pectin [12,13], alginate [14,15]), chemically adapted (chitosan [12,16,17], chitin [18]), or artificial (polyvinyl [19], polyacrylic acid [20,21], methacrylic acid [22], polystyrene [23], polyacrylamides [24], alkyl-trialkyl ammonium salts [22]). This technique allows the incorporation of other materials between polymer layers (biomolecules, nanoparticles).

Polyelectrolyte assembly is conducted on a sacrificial template core that easily decomposes in basic or acid media without affecting the polyelectrolyte capsule. The core can be fabricated from carbonates ($CaCO_3$, $CdCO_3$, $MnCO_3$) or oxides (SiO_2, TiO_2) [25–27]. The core can incorporate various materials (drugs, peptides, genes, or proteins) by preloading methods or can be dissolved once the capsules are fabricated, making room for drugs, peptides, genes, or proteins in so-called post-loading methods [28–31].

According to Robert Langer and Nikolaos Peppas, there are four types of drug delivery systems, depending on the mechanism of drug release: diffusion-controlled, chemically controlled, solvent-activated, and stimuli-controlled [32].

The polyelectrolyte microcapsules are sensitive to various external stimuli such as ultrasound, light, pH, and temperature, causing an increase in the permeability of the capsule shell and thus releasing the entrapped material [33–35]. The incorporation of magnetic nanoparticles had a beneficial influence on the characteristics of the capsules (increased responsiveness to stimuli, densifying the shells [36], and external manipulation of capsules by magnetic field [37–40]).

One of the challenges of drug targeting is the delivery of the drug to the point of interest, under safe conditions. The use of a magnetic field for this purpose is an easy and elegant method. A magnetic field is well suited for biological applications, as it is not shielded by biological fluids and does not interfere with most biological processes [41].

The literature includes many studies regarding the fabrication of various drug delivery systems exhibiting magnetic properties [42–44]. Materials such as synthetic polyelectrolytes and natural polymers (polysaccharides, polypeptides and polynucleotides, lipids, and multivalent dyes) can be used as layer constituents to fabricate the shells [45–47]. By incorporating various particles such as magnetite, iron, nickel, and cobalt, the drug carriers are attracted to a magnetic field [48,49].

Investigation of microcapsule movement and navigation is very important from fundamental and practical points of view. The characteristics of microcapsules containing iron oxide as one of the layers, as well as their alignment in a magnetic field, are well described in the literature [37,41,50]. The principle of drug delivery by a magnetic carrier is based on the use of both constant and high-frequency oscillating magnetic fields. In magnetically targeted therapy, a cytotoxic drug is attached to a biocompatible magnetic nanoparticle carrier [51]. These drug carriers are injected into the patient via the circulatory system. When the particles have entered the bloodstream, external, high-gradient magnetic fields are used to concentrate the drug carriers at a specific target site within the body.

Zebli et al. [52] demonstrated the accumulation of microcapsules and uptake by the cells present in the immediate vicinity. After 4 h of incubation, the internalization of capsules by cells located just above the edge of the permanent magnet drastically increased, compared to the distant cells. HeLa cells were incubated with a homogeneous mixture of fluorescent capsules in blue, green, red, and violet to demonstrate the feasibility of simultaneously loading cells with a variety of encapsulated cargos. The loading of cells was performed by adding magnetic nanoparticles into the wall of the capsules and trapping the capsules in a specific site by using a permanent magnet [53]. Kolesnikova studied microcapsule deposition in a blood-like viscous media. Various concentrations of glycerol in water have been used as liquid media for magnetic microcapsules. The authors concluded that capsule sedimentation time depends linearly on the medium viscosity [54].

Our group was involved in a project regarding the development of a more targeted methodology of developing cancer drugs using high-intensity focused ultrasound (HIFU) [55,56]. One of the issues was the transportation of capsules and their accumulation in the point of interest (i.e., tumor cells). For the supplementation of these investigations, we introduced an artery model for the examination of microcapsule behavior in an artificial vessel-like system. The magnetic field should be able to drive the magnetic capsules in the body; thus, choosing the ideal magnet system for a specific purpose is an important issue [57]. There are many studies of mathematical modeling investigating the parameters related to the capture efficiency of the magnetic particles [58,59]. A single permanent magnet is the simplest system for magnetic drug targeting. Due to the attractive force caused by the permanent magnet, more than 90% of the capsules containing magnetic nanoparticles were captured in the region near the magnet.

2. Materials and Method

2.1. Materials

Polystyrene sulfonate (PSS, 70 kDa), polyallylamine hydrochloride (PAH, 15 kDa), rhodamine B isothiocyanate (RBITC), calcium chloride, sodium carbonate, sodium chloride, bovine serum albumin (BSA), ethylenediaminetetraacetic acid (EDTA), and iron oxide (Fe_2O_3, Ø 50 nm) were purchased from Sigma-Aldrich, Gillingham, UK. Superparamagnetic iron oxide (Fe_3O_4, Ø 15 nm) was purchased from Skyspring Nanomaterials Inc., Houston, TX, USA. Bovine serum plasma was purchased from VWR, Lutterworth, UK and kept at −20 °C until use. All chemicals were used as received. Milli-Q Plus water (Sigma-Aldrich, Gillingham, UK), was used in all experiments.

2.2. Capsule Preparation

Fluorescent-labeled BSA was prepared by mixing 100 mg of BSA with 40 mL borate buffer (pH 9) and 1 mg of RBITC dissolved in 5 mL of ethanol for 12 h followed by 72 h dialysis against distilled water. Fluorescent-labeled BSA was captured within the $CaCO_3$ template core, prepared in situ by precipitation: 4 mL of BSA-RBITC solution was magnetically mixed with 10 mL of 0.33 M calcium chloride solution for five minutes at room temperature at 1000 rpm. Ten milliliters of 0.33 M sodium carbonate solution was added dropwise in one minute and the mixture was stirred for five minutes at room temperature. The solution was centrifuged at 5000 rpm for five minutes and the supernatant was discarded. The precipitate was washed with distilled water twice.

A solution of PAH (18 mL, 0.2 M in 0.5 M sodium chloride) was added to the core precipitate and the mixture was stirred at room temperature for 15 min, then centrifuged, and the supernatant was discarded. The precipitate was washed twice with distilled water.

A solution of PSS (18 mL, 0.2 M in 0.5 M sodium chloride) was added to the previous precipitate and the mixture was magnetically stirred (1000 rpm) at room temperature for 15 min, then centrifuged, and the supernatant was discarded. The precipitate was washed twice with distilled water. The particles are coated with two oppositely charged polyelectrolyte layers. The capsules were coated with a total of 12 layers.

The calcium carbonate template core was dissolved after deposition of 12 layers by mixing with chelating reagent EDTA (10 mL, 0.2 M solution) for 10 min followed by washing. The capsules were suspended in 20 mL of distilled water and analyzed.

2.3. Addition of Nanoparticles

Ferric oxide nanoparticles (Fe_2O_3, Ø 50 nm) or superparamagnetic iron oxide nanoparticles (Fe_3O_4, Ø 15 nm) 0.25 mg/mL were dispersed in 0.5 M sodium chloride solution by sonication in an ultrasonic bath (Langford Sonoma tic, 575, 40 kHz, 150 W power) for 30 min and used as one of the coating layers in the capsules' fabrication after PAH layer followed by the negatively charged PSS.

2.4. Transportation

Capsules were suspended in different media: distilled water, saline (9 mg/L), and bovine serum plasma in a concentration of 10^8 caps/mL. The suspension was transported by a peristaltic pump with a flow of 138 mL/h (2.3 mL/min) through a tube (20 mm × Ø 2 mm) over a permanent magnet (neodymium −12 kg force) with a diameter Ø 20 mm and a height of 10 mm. Experimental design is presented in Figure 1.

Preliminary tests revealed that passing the suspension over the magnet for more than one minute leads to clogging. Therefore, each experiment had a total duration of one minute. The volume of accumulated suspension was 0.0628 mL. The accumulated suspension was diluted in the working liquid and analyzed. The experiments were done in triplicates and average data and standard deviation are presented.

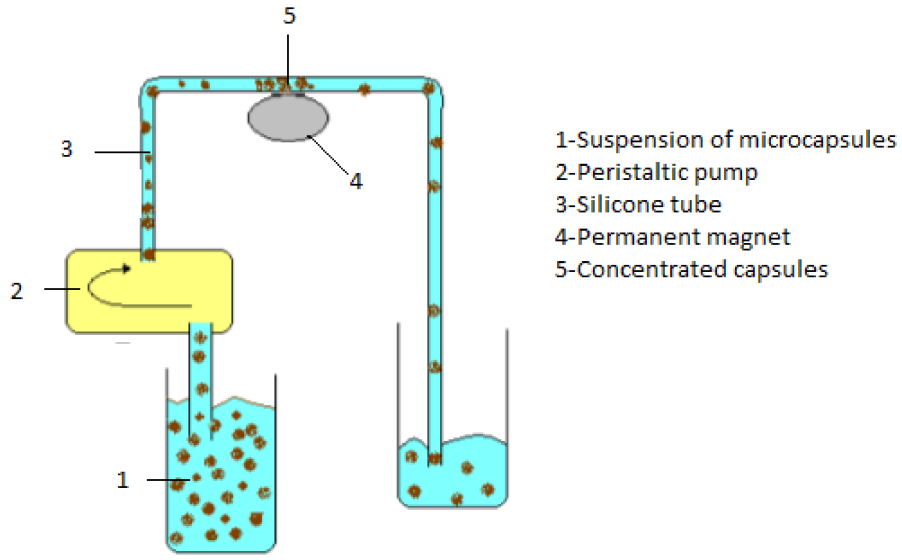

Figure 1. Experimental design: the microcapsules accumulate in the tube above the magnet.

3. Analysis

3.1. Capsule Size Distribution

A Malvern Multisizer 2000 laser diffractometer with a Hydro 2000 MU attachment (Malvern Instruments Ltd., Malvern, UK) was used to measure the particle size distribution of various capsules prepared by our standard protocol in the diameter range 0.38–500 µm.

3.2. Iron Content

The capsule suspension was digested in 5 mL hot HNO_3:HCl solution (1:1 v/v) for 15 min, and the iron concentration was determined using an inductively coupled plasma optical emission spectrometer (ICP-OES) Perkin Elmer Optima 5300DV (Perkin Elmer Inc., Hopkinton, MA, USA).

3.3. Accumulation/Depletion

The accumulated suspension was diluted 20 times. The depleted suspension was analyzed with no further dilutions.

The number of accumulated/depleted capsules was counted by using a hemocytometer chamber. The accumulation of capsules was calculated according to the equation:

$$\text{Acc (\%)} = 100 - (\text{Ci}/\text{Cd})$$

where:

- Acc is the accumulated percentage of capsules within the portion of the tube placed on the top of the magnet;
- Ci is the concentration of capsules at the entry point in the peristaltic pump;
- Cd is the concentration of the capsules after passing over the permanent magnet.

4. Results and Discussions

Microcapsules consisting of 11 layers of polyelectrolyte and 1 layer of iron oxide nanoparticles were fabricated and tested as possible drug delivery systems for solid tumors. HIFU, currently used in cancer surgery, was used as a remote tool for the rupture of microcapsules and release of the content [55,56]. In order to capture the drug carriers at the tumor site, a simple cylindrical tube system passing over a permanent magnet was used to track the trajectory of magnetic particles under a laminar flow.

Two types of nanoparticles were inserted as one of the layers within the microcapsule's walls: Fe_2O_3, ferric oxide, having Ø 50 nm and superparamagnetic Fe_3O_4 having Ø 15 nm (Figure 2).

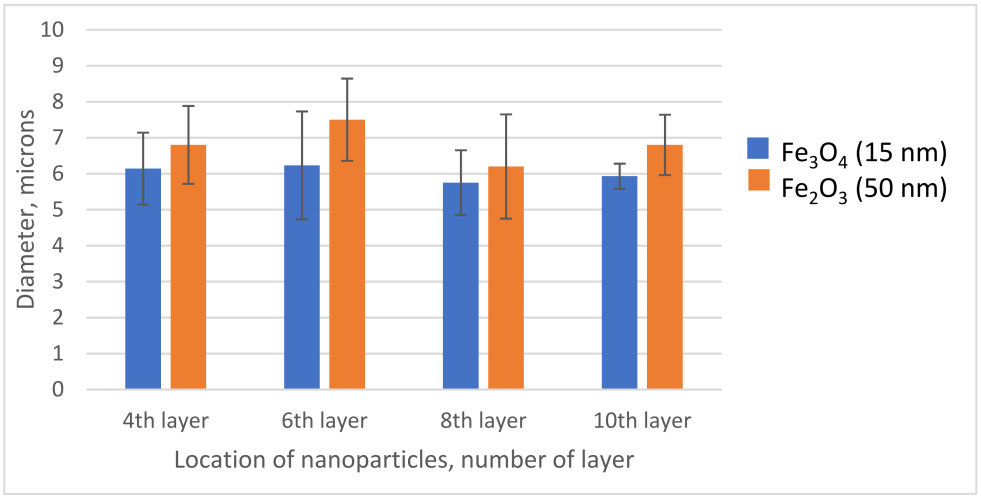

Figure 2. Mean diameter of microcapsules.

The iron amount in each type of capsules was determined by ICP-OES after the complete chemical breakdown of the shells and acid digestion of the iron oxide nanoparticles. The content of iron oxide was normalized to 100 million (10^{10}) capsules taking into consideration the concentration of capsules in suspension (Table 1).

Table 1. Iron content in microcapsules (μg/10^{10} capsules).

Location of Nanoparticles	Type of Nanoparticle	
	Fe_3O_4 (Ø 15 nm)	Fe_2O_3 (Ø 50 nm)
4th layer	1.75	2.31
6th layer	1.56	2.36
8th layer	1.69	1.87
10th layer	1.19	1.71

By using a peristaltic pump, the capsule suspension was circulated through a very thin tube into a recipient. The permanent magnet was placed under the tube at the middle distance between the pump and the recipient vial (Figure 1).

The model system chosen in the experiments simulates an interaction of two forces: movement of the capsules when pumped through the tube and manipulation of capsules by a permanent magnet. The flow mimics the bloodstream in the circulatory system, while the magnetic field gradient allows for the concentration of capsules loaded with magnetic nanoparticles at a specific place.

Various types of mathematical models have been proposed for the behavior of magnetic particles in a magnetic field. Semianalytical expressions to quantify the number of captured particles as a function of distance were found to provide good first-order approximations. Reasonable agreement was found between the measured trajectories and numerical predictions [57–59]. Variations in particle size and magnetic loading also contributed to the distribution in particle position about the projected trajectory.

Under flow, the capsules were captured by the magnetic field and were accumulated in the flow channel, at the area of the location of the magnet. In this region, their concentration drastically increased. The concentration of nanoparticles/capsules depends on the shape of the magnet, with the button magnet accumulating above the edges of the cylinder and the rod-type magnet accumulating at the leading edge. These designs have as practical applications cases where the capsules need to be delivered to a diffuse area [59]. This illustrates a method for the magnetic delivery of polymer capsules loaded with pharmaceutical agents such as doxorubicin and 5-fluorouracil [60–64]. Similar systems have been used by

Alexiou in cancer therapy; when using starch-coated magnetic nanoparticles, about 90% accumulation near a permanent magnet was observed [65].

The initial capsule distribution in the vial was quasi homogeneous and maintained in that state by agitation. Capsules were aligned into parallel stripes as they passed through the magnetic field (Figure 3).

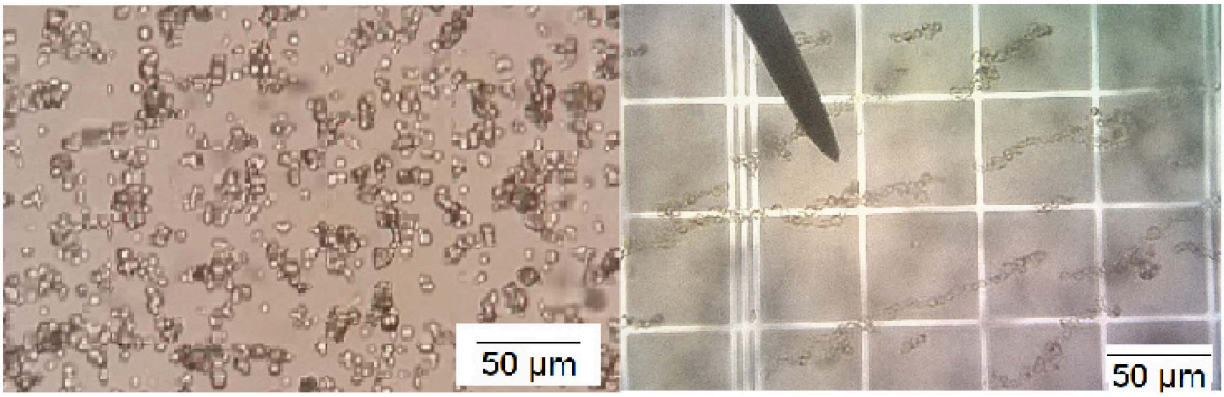

Figure 3. Capsules: (**left**) before passing over the magnet; (**right**) after passing over the magnet.

4.1. Capsules Containing Fe_2O_3

Distilled water was the working and washing medium during capsules' preparation. The microcapsules were stable in distilled water for up to several weeks.

The accumulation of capsules was quite high, exceeding 90% (Figure 4). There was a slight decrease in the accumulation of microcapsules containing ferric oxide as the nanoparticles were placed closer to the outer layer.

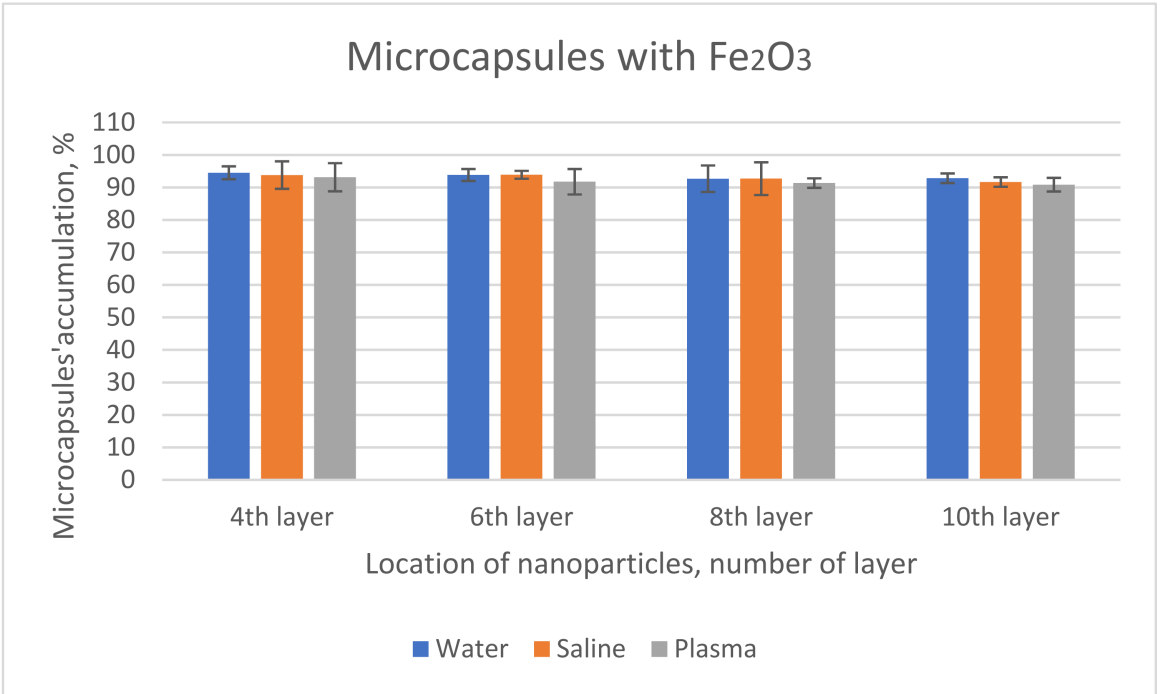

Figure 4. Accumulation of microcapsules containing Fe_2O_3 nanoparticles, %.

Physiological saline solution is 0.9% sodium chloride in water, with a density of 1.0046 g/cm^3; it is an excellent electrolyte for the cells, it has the same osmotic pressure as the body fluid, and it is the transportation media for parentally administered drugs. In

saline solution, the microcapsules containing ferric oxide showed a similar behavior as in water.

Bovine plasma is a complex electrolyte solution containing many proteins such as fibrinogen, albumin, and globulin in water. The proteins have some important functional properties such as solubility, foaming, and emulsification. The physical properties of bovine plasma depend on the concentration of proteins and pH [66,67]. Density of bovine plasma is 1.035 g/cm^3 and kinematic viscosity is 1.06–1.15 cP. Since plasma is the matrix of blood cells, the influence of plasma as a transportation media on the microcapsules crossing a magnetic field is of high interest.

4.2. Capsules Containing Fe_3O_4

Microcapsules containing magnetite also accumulated in a high amount (Figure 5). In water, the trend was similar to the other type of microcapsules; there was a slight decrease in the percentage of accumulation as the nanoparticles were placed closer to the outer layer. However, in saline and plasma, they tended to agglomerate as the nanoparticles were placed closer to the outer layer. Thus, the location of nanoparticles (close to the surface or, on the contrary, close to the core) exerts some influence.

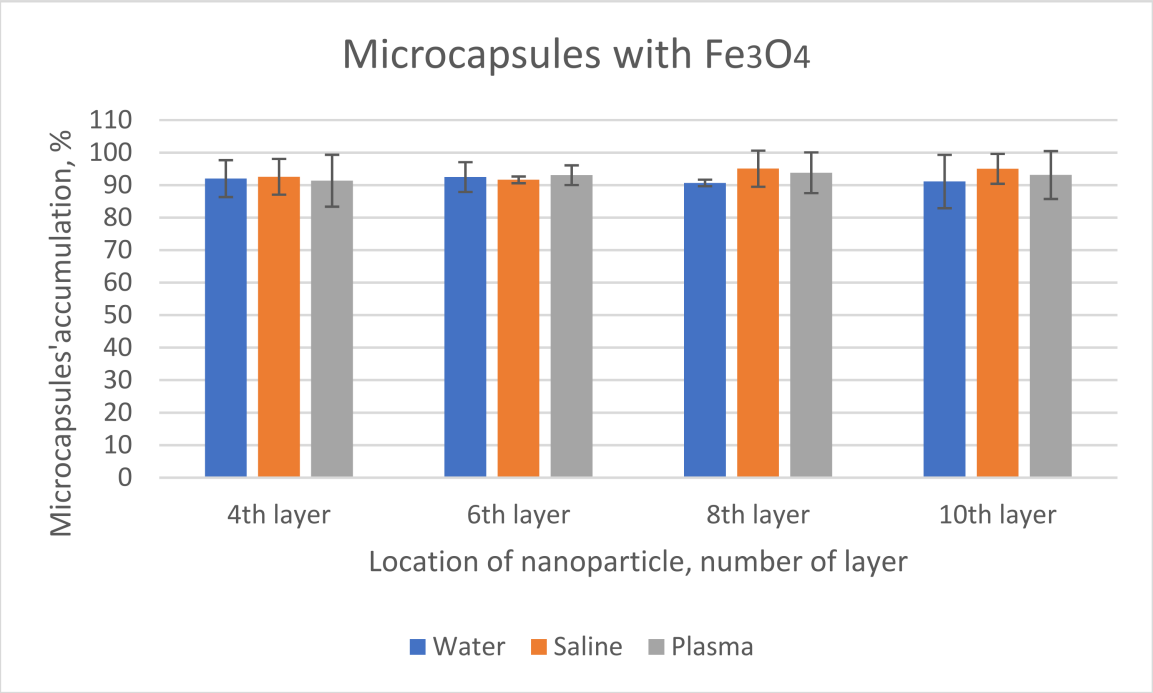

Figure 5. Accumulation of microcapsules with Fe_3O_4, %.

Obviously, the accumulation is mainly governed by the amount of iron oxide embedded within.

In the case of ferric oxide (Fe_2O_3, Ø 50 nm), a higher amount of iron was inserted in the capsules having iron oxide as the 4th and 6th layers, with a decrease in the amount of iron as the nanoparticles form the 8th and 10th layers, respectively. Thus, greater accumulation is observed when nanoparticles are placed on 4th and 6th layers as compared to 8th and 10th layers, regardless of the transportation fluid used.

Microcapsules with Fe_3O_4 embedded had also lower amounts of iron as the nanoparticles were placed close to the surface. However, in this case, the percentage of accumulation was rising. Other characteristics of the microcapsules as a whole act in this direction, besides the amount of embedded iron oxide. One property to be considered is the dimensions of the capsules. The microcapsules having ferric oxide embedded are bigger and probably heavier, and thus they move slower. Magnetite capsules have smaller sizes and thus are

easily captured in the magnetic field. Wicke et al. reached the same conclusion when using a mathematical model for the simulation of magnetic particles subject to fluid flow in a magnetic field [68].

Another factor that must be considered when moving objects is the density of the media. Thus, plasma is a much dense fluid than water, slowing the capsules circulating over the top of the magnet. Therefore, a lower accumulation rate should be observed than in the case when water was the transportation medium. This is true in the case of ferric oxide capsules, where the accumulation increases in the order bovine plasma < saline solution < distilled water, yet for magnetite the results are somewhat different. There is the same tendency regarding bovine plasma and saline solution, while in distilled water the number of captured capsules is lower.

5. Conclusions

The microcapsules prepared by LbL technique incorporating magnetic nanoparticles (Fe_2O_3, 50 nm, or Fe_3O_4, 15 nm) could be directed and concentrated, in a tube with a diameter similar to a blood vessel, using an external magnetic field. The accumulation was fast, and in less than a minute the concentration of capsules was more than 90% of the initial concentration, clogging the tube. These experiments proved that polymer capsules can be deposited in a specific spot. Therefore, polyelectrolyte magnetic capsules can be used as molecular communication devices carrying information while traveling through fluid media to deliver messages. Moreover, in cancer therapy, magnetic polyelectrolyte capsules containing cytostatic drugs can be injected close to a solid tumor and concentrated by means of a magnetic field, followed by the release of the drug by external stimuli such as light or ultrasound.

Author Contributions: Conceptualization, C.S, MV. and T.M.; validation, C.S., M.V. and T.M.; formal analysis, C.S., M.V., and T.M.; investigation, C.S.; resources, T.M; data curation, C.S., M.V. and T.M.; writing—original draft preparation, C.S.; writing—review and editing, M.V. and T.M.; visualization, M.V. and T.M.; supervision, M.V.; project administration, T.M.; funding acquisition, T.M.. All authors have read and agreed to the published version of the manuscript.

Funding: This research received no external funding.

Institutional Review Board Statement: Not applicable.

Informed Consent Statement: Not applicable.

Data Availability Statement: Not applicable.

Acknowledgments: This research has been funded by a number of charitable trusts, the largest donations coming from The James Tudor Foundation, William A Cadbury Charitable Trust, Carol's Smile, The Grace Fry Charitable Trust, The Sobell Foundation, and The Charles and Elsie Sykes Trust. Without their support, this research would not have been possible.

Conflicts of Interest: The authors declare no conflict of interest.

References

1. Jain, K.K. *Drug Delivery Systems in Methods in Molecular Biology*, 2nd ed.; Humana Press: Basel, Switzerland, 2014.
2. Siepmann, J.; Siegel, R.A.; Rathbone, M.J. *Fundamentals and Applications of Controlled Release Drug Delivery*; Springer: Cham, Switzerland, 2012.
3. Eloy, J.O.; Marchetti, J.M.; Abriata, J.P. *Nanocarriers for Drug Delivery: Concepts and Applications*; Springer: Cham, Switzerland, 2021.
4. Ruman, U.; Fakurazi, S.; Masarudin, M.J.; Hussein, M.Z. Nanocarrier-Based Therapeutics and Theranostics Drug Delivery Systems for Next Generation of Liver Cancer Nanodrug Modalities. *Int. J. Nanomed.* **2020**, *15*, 1437–1456. [CrossRef] [PubMed]
5. Hossen, S.; Hossain, M.K.; Basher, M.K.; Mia, M.N.H.; Rahman, M.T.; Uddin, M.J. Smart nanocarrier-based drug delivery systems for cancer therapy and toxicity studies: A review. *J. Adv. Res.* **2018**, *15*, 1–18. [CrossRef] [PubMed]
6. Jacob, J.; Haponiuk, J.T.; Thomas, S.; Gopi, S. Biopolymer based nanomaterials in drug delivery systems: A review. *Mater. Today Chem.* **2018**, *9*, 43–55. [CrossRef]
7. Atanase, L.I. Micellar Drug Delivery Systems Based on Natural Biopolymers. *Polymers* **2021**, *13*, 477. [CrossRef] [PubMed]
8. Jagtap, P.; Patil, K.; Dhatrak, P. Polyelectrolyte Complex for Drug Delivery in Biomedical Applications: A review. *IOP Conf. Ser. Mater. Sci. Eng.* **2021**, *1183*, 012007. [CrossRef]

9. Shama, V.; Sundaramurthy, A. Multilayer capsules made of weak polyelectrolytes: A review on the preparation, functionalization and applications in drug delivery. *Beilstein J. Nanotechnol.* **2020**, *11*, 508–532. [CrossRef]
10. Stoleru, E.; Vasile, C. Nucleic acids-based bionanomaterials for drug and gene therapy. In *Polymeric Nanomaterials in Nanotherapeutics*; Cornelia, V., Ed.; Elsevier: Amsterdam, The Netherlands, 2019; Chapter 6; pp. 235–260.
11. Ruesing, J.; Rotan, O.; Gross-Heitfeld, C.; Mayer, C.; Epple, M. Nanocapsules of a cationic polyelectrolyte and nucleic acid for efficient cellular uptake and gene transfer. *J. Mater. Chem. B* **2014**, *2*, 4625–4630. [CrossRef]
12. Wang, H.; Yang, B.; Sun, H. Pectin-Chitosan Polyelectrolyte Complex Nanoparticles for Encapsulation and Controlled Release of Nisin. *Am. J. Polym. Sci. Technol.* **2017**, *3*, 82–88. [CrossRef]
13. Ji, F.; Li, J.; Qin, Z.; Yang, B.; Zhang, E.; Dong, D.; Wang, J.; Wen, Y.; Tian, L.; Yao, F. Engineering pectin-based hollow nanocapsules for delivery of anticancer drug. *Carbohydr. Polym.* **2017**, *177*, 86–96. [CrossRef]
14. Roy, S.; Elbaz, N.M.; Parak, W.J.; Feliu, N. Biodegradable Alginate Polyelectrolyte Capsules as Plausible Biocompatible Delivery Carriers. *ACS Appl. Biol. Mater.* **2019**, *2*, 3245–3256. [CrossRef]
15. Boi, S.; Rouatbi, N.; Dellacasa, E.; Di Lisa, D.; Bianchini, P.; Monticelli, O.; Pastorino, L. Alginate microbeads with internal microvoids for the sustained release of drugs. *Int. J. Biol.* **2020**, *156*, 454–461. [CrossRef] [PubMed]
16. Morin-Crini, N.; Lichtfouse, E.; Torri, G.; Crini, G. Fundamentals and Applications of Chitosan. *Sustain. Agric. Rev.* **2019**, *35*, 49–123.
17. Ejeromedoghene, O.; Oderinde, O.; Egejuru, G.; Adewuyi, A. Chitosan-drug encapsulation as a potential candidate for COVID-19 drug delivery systems: A review. *JOTCS* **2020**, *7*, 851–864. [CrossRef]
18. Rinaudo, M.; Kil'deeva, N.R.; Babak, V.G. Surfactant-polyelectrolyte complexes on the basis of chitin. *Russ. J. Gen. Chem.* **2008**, *78*, 2239–2246. [CrossRef]
19. Chen, W.; Zhou, S.; Ge, L.; Wu, W.; Jiang, X. Translatable High Drug Loading Drug Delivery Systems Based on Biocompatible Polymer Nanocarriers. *Biomacromolecules* **2018**, *19*, 1732–1745. [CrossRef]
20. Zakharova, L.Y.; Vasilieva, E.A.; Gaynanova, G.A.; Mirogorodska, A.B.; Ibragimova, A.R.; Salnikov, V.V.; Uchegbu, I.F.; Konovalov, A.I.; Zuev, Y.F. The polyacrylic acid/modified chitosan capsules with tunable release of small hydrophobic probe and drug. *Colloids Surf.* **2015**, *471*, 93–100. [CrossRef]
21. Kinnane, C.R.; Such, G.K.; Caruso, F. Tuning the Properties of Layer-by-Layer Assembled Poly(acrylic acid) Click Films and Capsules. *Macromolecules* **2011**, *44*, 1194–1202. [CrossRef]
22. Burke, N.A.D.; Mazumder, M.A.J.; Hanna, M.; Stover, H.D. Polyelectrolyte Complexation Between Poly(methacrylic acid, sodium salt) and Poly(diallyldimethylammonium chloride) or Poly[2-(methacryloyloxyethyl)trimethylammonium chloride]. *J. Polym. Sci. Part A Polym. Chem.* **2007**, *45*, 4129–4143. [CrossRef]
23. Skirtach, A.G.; Yashchenok, A.M.; Mohwald, H. Encapsulation, release and applications of LbL polyelectrolyte multilayer capsules. *Chem. Commun.* **2011**, *47*, 12736–12746. [CrossRef]
24. Lilienthal, S.; Fischer, A.; Liao, W.-C.; Cazelles, R.; Willner, I. Single and Bilayer Polyacrylamide Hydrogel-Based Microcapsules for the Triggered Release of Loads, Logic Gate Operations, and Intercommunication between Microcapsules. *ACS Appl. Mater. Interfaces* **2020**, *12*, 31124–31136. [CrossRef]
25. Antipov, A.A.; Sukhorukov, G.B. Polyelectrolyte multilayer capsules as vesicles with tunable permeability. *Adv. Colloid Interface Sci.* **2004**, *11*, 49–61. [CrossRef]
26. Da Silva Abreu, A.; Carvalho, J.A.; Tedesco, A.C.; Beltrame, M.; Simioni, A.R. Fabrication of polyelectrolyte microspheres using porous manganese carbonate as sacrifical template for drug delivery application. *J. Mater. Res.* **2019**, *34*, 1353–1362. [CrossRef]
27. Cui, X.; Chen, H.; Ye, Q.; Cui, X.; Cui, X.; Cui, H.; Shen, G.; Lin, J.; Sun, Y. Porous Titanium Dioxide Sphere for Drug Delivery and Sustained Release. *Front. Mater.* **2021**, *8*, 204. [CrossRef]
28. Yang, Q.; Li, L.; Zhao, F.; Wang, Y.; Ye, Z.; Hua, C.; Liu, Z.; Bohnic, K.; Guo, X. Spherical Polyelectrolyte Brushes as Templates to Prepare Hollow Silica Spheres Encapsulating Metal Nanoparticles. *Nanomaterials* **2020**, *10*, 799. [CrossRef]
29. Nguyen, N.T.; Dao, T.H.; Truong, T.T.; Nguyen, T.M.T.; Pham, T.D. Adsorption characteristic of ciprofloxacin antibiotic onto synthesized alpha alumina nanoparticles with surface modification by polyanion. *J. Mol. Liq.* **2020**, *309*, 113150–113158. [CrossRef]
30. Agdel-Bary, A.S.; Tolan, D.A.; Nassar, M.Y.; Taketsugu, T.; El-Nahas, A.M. Chitosan, magnetite, silicon dioxide, and graphene oxide nanocomposites: Synthesis, characterization efficiency as cisplatin drug delivery, and DFT calculations. *Int. J. Biol.* **2020**, *154*, 621–633.
31. Anirudhan, T.S.; Chithra Sekhar, V.; Nair, S.S. Polyelectrolyte complexes of carboxymethyl chitosan/alginate based drug carrier for targeted and controlled release of dual drug. *J. Drug Deliv. Sci. Technol.* **2019**, *51*, 569–582. [CrossRef]
32. Langer, R.; Peppas, N. Chemical and physical structure of polymers as carriers for controlled release of bioactive agents: A review. *J. Macromol. Sci. Phys.* **1983**, *23*, 61–126. [CrossRef]
33. Antipina, M.N.; Sukhorukov, G.B. Remote control over guidance and release properties of composite polyelectrolyte-based capsules. *Adv. Drug Deliv. Rev.* **2011**, *63*, 716–729. [CrossRef]
34. Delcea, M.; Mohwald, H.; Skirtach, A.G. Stimuli-responsive LbL capsules and nanoshells for drug delivery. *Adv. Drug Deliv. Rev.* **2011**, *63*, 730–747. [CrossRef]
35. Fomina, N.; Sankaranarayanan, J.; Almutairi, A. Photochemical mecanisms of light-triggered release from nanocarriers. *Adv. Drug Deliv. Rev.* **2012**, *64*, 1005–1020. [CrossRef] [PubMed]

36. Lomova, M.V.; Brichkina, A.I.; Kiryukhin, M.V.; Vasina, E.N.; Pavlov, A.M.; Gorin, D.A.; Sukhorukov, G.B.; Antipina, M.N. Multilayer Capsules Of Bovine Serum Albumin and Tannic Acid for Controlled Release by Enzymatic Degradation. *ACS Appl. Mater. Interfaces* **2015**, *7*, 11732–11740. [CrossRef] [PubMed]
37. Gaponik, N.; Radtchenko, I.L.; Sukhorukov, G.B.; Rogach, A.L. Luminescent Polymer Microcapsules Addressable by a Magnetic Field. *Langmuir* **2004**, *20*, 1449–1452. [CrossRef]
38. Hu, S.H.; Tsai, C.H.; Liao, C.F.; Liu, D.M.; Chen, S.Y. Controlled Rupture of Magnetic Polyelectrolyte Microcapsules for Drug Delivery. *Langmuir* **2008**, *24*, 11811–11818. [CrossRef]
39. Fang, M.; Grant, P.S.; McShane, M.J.; Sukhorukov, G.B.; Golub, V.O.; Lvov, Y.M. Magnetic Bio/Nanoreactor with Multilayer Shells of Glucose Oxidase and Inorganic Nanoparticles. *Langmuir* **2002**, *18*, 6338–6344. [CrossRef]
40. Liu, J.F.; Jang, B.; Issadore, D.; Tsourkas, A. Use of magnetic fields and nanoparticles to trigger drug release and improve tumor targeting. *Wiley Interdiscip. Rev. Nanomed. Nanobiotechnol.* **2019**, *11*, e1571. [CrossRef]
41. Carregal-Romero, S.; Guardia, P.; Yu, X.; Hartmann, R.; Pellegrino, T.; Parak, W.J. Magnetically triggered release of molecular cargo from iron oxide nanoparticle loaded microcapsules. *Nanoscale* **2015**, *7*, 570–576. [CrossRef]
42. Ridi, F.; Bonini, M.; Baglioni, P. Magneto-responsive nanocomposites: Preparation and integration of magnetic nanoparticles into films, capsules, and gels. *Adv. Colloid Interface Sci.* **2014**, *207*, 3–13. [CrossRef]
43. Martina, M.-S.; Fortin, J.-P.; Fornier, L.; Menager, C.; Gazeau, F.; Clement, O.; Lesieur, S. Magnetic Targeting of Rhodamine-Labeled Superparamagnetic Liposomes to Solid Tumors: In Vivo Tracking by Fibered Confocal Fluorescence Microscopy. *Mol. Imaging* **2007**, *6*, 140–146. [CrossRef]
44. Yang, H.Y.; Li, Y.; Lee, S.S. Multifunctional and Stimuli-Responsive Magnetic Nanoparticle-Based Delivery Systems for Biomedical Applications. *Adv. Therap.* **2018**, *1*, 1800011. [CrossRef]
45. Nishida, K. Recent Advances in Lipid-Based Drug Delivery. *Pharmaceutics* **2021**, *13*, 926. [CrossRef] [PubMed]
46. Fiejdasz, S.; Gilarska, A.; Horak, W.; Radziszewska, A.; Straczek, T.; Szuwarzynski, M.; Nowakowska, M.; Kapusta, C. Structurally stable hybrid magnetic materials based on natural polymers-preparation and characterization. *J. Mater. Sci. Technol.* **2021**, *15*, 3149–3160. [CrossRef]
47. Tataru, G.; Popa, M.; Desbrieres, J. Magnetic microparticles based on natural polymers. *Int. J. Pharm.* **2011**, *404*, 83–93. [CrossRef] [PubMed]
48. Mannu, R.; Karthikeyan, V.; Velu, N.; Arumugam, C.; Roy, V.A.L.; Gopalan, A.-J.; Saianand, G.; Sonar, P.; Lee, K.-P.; Kim, W.-J.; et al. Polyethylene Glycol Coated Magnetic Nanoparticles: Hybrid Nanofluid Formulation, Properties and Drug Delivery Prospects. *Nanomaterials* **2021**, *1*, 440. [CrossRef] [PubMed]
49. Al-Musawi, S.; Ibraheem, S.; Mahdi, S.A.; Albukhaty, S.; Haider, A.J.; Kadhim, A.A.; Kadhim, K.A.; Kadhim, H.A.; Al-Karagoly, H. Smart Nanoformulation Based on Polymeric Magnetic Nanoparticles and Vincrisitine Drug: A Novel Therapy for Apoptotic Gene Expression in Tumors. *Life* **2021**, *11*, 71. [CrossRef] [PubMed]
50. Luo, D.; Poston, R.N.; Gould, D.J.; Sukhorukov, G.B. Magnetically targetable microcapsules display subtle changes in permeability and drug release in response to a biologically comppatible low frequency alternating magnetic field. *Mater. Sci. Eng. C* **2019**, *94*, 647–655. [CrossRef] [PubMed]
51. Saini, R.K.; Chouhan, R.; Bagri, L.P.; Bajpai, A.K. Strategies of Targeting Tumors and Cancers. *J. Cancer Res. Updates* **2012**, *1*, 129–152.
52. Zebli, B.; Susha, A.S.; Sukhorukov, G.B.; Rogach, A.L.; Parak, W.J. Magnetic Targeting and Cellular Uptake of Polymer Microcapsules Simultaneously Functionalized with Magnetic and Luminescent Nanocrystals. *Langmuir* **2005**, *21*, 4262–4265. [CrossRef]
53. Ochs, M.; Carregal-Romero, S.; Rejman, J.; Braeckmans, K.; De Smedt, S.C.; Parak, W.J. Light-Addressable Capsules as Caged Compound Matrix for Controlled Triggering of Cytosolic Reactions. *Angew. Chem. Int. Ed.* **2013**, *52*, 695–699. [CrossRef]
54. Kolesnikova, T.A.; Akchurin, G.G.; Portnov, S.A.; Khomutov, G.B.; Akchurin, G.G.; Naumova, O.G.; Sukhorukov, G.B.; Gorin, D.A. Visualization of magnetic microcapsules in liquid by optical coherent tomography and control of their arrangement via external magnetic field. *Laser Phys. Lett.* **2012**, *9*, 643–648. [CrossRef]
55. Stavarache, C.E. Paniwnyk, Controlled rupture of magnetic LbL polyelectrolyte capsules and subsequent release of contents employing high intensity focused ultrasound. *J. Drug. Deliv. Sci. Technol.* **2018**, *45*, 60–69. [CrossRef]
56. Stavarache, C.; Vinatoru, M.; Mason, T. The Effect of Focused Ultrasound on Magnetic Polyelectrolyte Capsules Loaded with Dye When Suspended in Tissue-Mimicking Gel. *Curr. Drug Deliv.* **2019**, *16*, 355–363. [CrossRef]
57. Liu, Y.-L.; Chen, D.; Shang, P.; Yin, D.-C. A review of magnet systems for targeted drug delivery. *J. Control. Release* **2019**, *302*, 90–104. [CrossRef] [PubMed]
58. Barnsley, L.C.; Carugo, D.; Aron, M.; Stride, E. Understanding the dynamics of superparamagnetic particles under the influence of high field gradient arrays. *Phys. Med. Biol.* **2017**, *62*, 2333–2360. [CrossRef] [PubMed]
59. Sharma SSingh, U.; Katiyar, V.K. Magnetic field effect on flow parameters of blood along with magnetic particles in a cylindrical tube. *J. Magn. Magn. Mater.* **2015**, *377*, 395–401. [CrossRef]
60. Gunasekera, U.A.; Pankhurst, Q.A.; Douek, M. Imaging applications of nanotechnology in cancer. *Target. Oncol.* **2009**, *4*, 169–181. [CrossRef]
61. Entezar-Almahdi, E.; Mohammadi-Samani, S.; Tayebi, L.; Farjadian, F. Recent Advances in Designing 5-Fluorouracil Delivery Systems: A Stepping Stone in the Safe Treatment of Colorectal Cancer. *Int. J. Nanomed.* **2020**, *15*, 5445–5458. [CrossRef]

62. Lince, F.; Bolognesi, S.; Stella, B.; Marchisio, D.L.; Dosio, F. Preparation of polymer nanoparticles loaded with doxorubicin for controlled drug delivery. *Chem. Eng. Res. Des.* **2011**, *89*, 2410–2419. [CrossRef]
63. Babos, G.; Biro, E.; Meiczinger, M.; Feczko, T. Dual Drug Delivery of Sorafenib and Doxorubicin from PLGA and PEG-PLGA Polymeric Nanoparticles. *Polymers* **2018**, *10*, 895. [CrossRef]
64. Manshadi, M.K.; Saadat, M.; Mohammadi, M.; Shamsi, M.; Dejam, M.; Kamali, R.; Sanati-Nezhad, A. Delivery of magnetic micro/nanoparticles and magnetic-based drug/cargo into arterial flow for targeted therapy. *Drug Deliv.* **2018**, *25*, 1963–1973. [CrossRef]
65. Seliger, C.; Jurgons, R.; Wiekhorst, F.; Eberbeck, D.; Trahms, L.; Iro, H.; Alexiou, C. In vitro investigation of the behaviour of magnetic particles by a circulating artery model. *J. Magn. Magn. Mater.* **2007**, *311*, 358–362. [CrossRef]
66. Opoku, A.; Tabil, L.G.; Crerar, B. Rheological and physical properties of bovine plasma fibriogen-enriched plasma. Presented at the CSAE/SCGR 2005 Meeting, Winnipeg, Manitoba, 26–29 June 2005.
67. Howell, N.K.; Lawrie, R.A. Functional aspects of blood plasma proteins: V. Viscosity. *Int. J. Food Sci. Technol.* **2007**, *22*, 145–151. [CrossRef]
68. Wicke, W.; Ahmadzadeh, A.; Jamali, V.; Schober, R.; Unterweger, H.; Alexiou, C. Molecular Communication using Magnetic Nanoparticles. In Proceedings of the 2018 IEEE Wireless Communications and Networking Conference (WCNC), Barcelona, Spain, 15–18 April 2018.